Melt spinning of crystalline alloys

Rapid solidification techniques have been studied ever since the early experiments of Duwez *et al.* [1, 2]. In recent years, the melt-spinning process (sometimes known as chill block casting) has been of particular interest because of the possibility of manufacturing iron-based amorphous alloys for magnetic applications [2]. Liebermann and Graham [3] and Kavesh [4] have discussed the effect of melt-spinning process parameters on the dimensions of melt-spun ribbons of amorphous $Fe_{40}Ni_{40}B_{20}$. This note describes the results of an investigation into the effect of melt spinning process parameters on the ribbon dimensions of two other materials, namely Pb–Sn eutectic and Al containing small quantities of Fe and Mn. The main objective was to determine whether the conclusions of Liebermann and Graham and Kavesh can be applied over a wide range of materials. Thus, Pb–Sn and Al–(Fe,Mn) were chosen because they have very different melting points from $Fe_{40}Ni_{40}B_{20}$, and because they solidify in a crystalline rather than amorphous form.

Master alloys of Pb–Sn eutectic, Al–2 wt%Fe, and Al–2 wt%Mn were prepared by induction melting 99.99% pure components in recrystallized alumina crucibles under a dynamic argon atmosphere melt-spun ribbons were produced as follows. Each specimen of 2 to 3 g was placed in a 9 mm diameter quartz tube at the bottom of which was a small orifice. After flushing the tube with argon the specimen was induction melted, and then ejected by argon slightly above atmospheric pressure on to a rapidly rotating, highly polished copper drum to produce a melt-spun ribbon. Ribbons were prepared with ejection pressures in the range of ~ 5 to 40 kPa above atmospheric pressure with orifice diameters from ~ 0.75 to 1.50 mm, and with drum surface velocities between ~ 4 to 30 m sec^{-1}.

The resulting melt-spun ribbons of Pb–Sn eutectic consisted of equiaxed Pb and Sn rich grains ~ 4 μm in diameter, and exhibited superplastic behaviour when subjected to a tensile stress. The microstructure and mechanical properties of melt-spun Pb–Sn eutectic ribbons have been discussed in detail elsewhere [5]. The microstructure of melt-spun Al alloys was not investigated, but X-ray diffractometry showed the presence of the Al together with a small amount of an unidentified second phase. To determine the effect of melt-spinning process parameters on ribbon dimensions, the width of Pb–Sn and Al alloy ribbons was determined with a travelling microscope. The Pb–Sn eutectic ribbons had sufficiently smooth surfaces that a satisfactory measurement of their thickness could be obtained by direct measurement with a micrometer. For the Al alloys however, the surfaces were too rough so that the thickness had to be measured by weighing a known length of ribbon and using the expression $t = W/lw\rho$ where l, w, t are ribbon length, width and thickness, ρ is density (2.71×10^3 Kgm^{-3}), and W is the measured weight.

Liebermann and Graham [3] applied Bernoulli's equation, essentially an energy balance, to the column of liquid metal during ejection from the orifice. Bernoulli's equation is $V_J^2 = 2P/\rho$ where V_J is the velocity of the liquid jet leaving the orifice and P is the ejection pressure, and the continuity equation for an incompressible fluid gives the volumetric flow rate $Q = A_R V_R = A_J V_J$ where A_R, A_J are cross-sectional areas of ribbon and jet respectively and V_R is the ribbon velocity. These two equations can be combined, putting the ribbon velocity V_R equal to the surface velocity of the drum, V_S, and taking the cross-sectional area of the jet $A_J = \pi\Phi^2/4$ where Φ is the orifice dia-

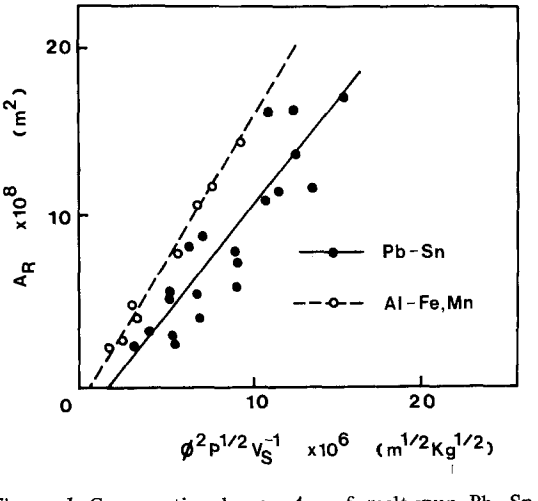

Figure 1 Cross-sectional area A_R of melt-spun Pb–Sn eutectic and Al alloy ribbons as a function of orifice diameter Φ, ejection pressure P, and surface velocity of the drum V_S, following the analysis of Liebermann and Graham [3]. The points are experimental data and the lines show the least-squares best fit.

0022–2461/80/102658–04 $02.40/0

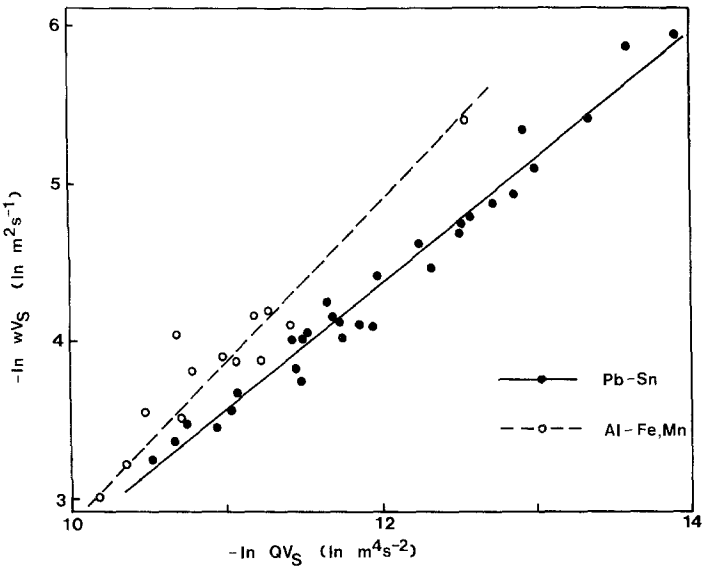

Figure 2 Ribbon width w for melt-spun Pb–Sn eutectic and Al alloys as a function of volumetric flow rate Q and surface velocity of the drum V_S, following the analysis of Kavesh [4]. The points show the experimental data and the lines show the least-squares best fit.

meter. This leads to

$$A_R = \pi\Phi^2 P^{1/2}/2^{3/2} V_S \rho^{1/2} \quad (1)$$

Equation 1 can be generalized to allow for energy losses in the orifice by incorporating a discharge co-efficient C_D so that $V_J^2 = 2C_D^2 P/\rho$ and

$$A_R = \pi C_D \Phi^2 P^{1/2}/2^{3/2} V_S \rho^{1/2} \quad (2)$$

Liebermann and Graham found a good fit to Equation 2 for amorphous ribbons of $Fe_{40}Ni_{40}B_{20}$ taking $C_D = 1$. The present results for Pb–Sn eutectic and Al–2%(Fe,Mn) are shown in Fig. 1 as a plot of A_R versus $\Phi^2 P^{1/2}/V_S$. The results agree quite well with the linear relationship expected from Equation 2, although there is some scatter in the Pb–Sn data possibly because of the poorer method of measuring thickness. Linear regression analysis gives a slope for Pb–Sn eutectic of 1.23×10^{-2} m$^{3/2}$ kg$^{-1/2}$ with a correlation coefficient of 0.90; for the Al alloys the slope is 1.63×10^{-2} m$^{3/2}$ kg$^{-1/2}$ with a correlation coefficient of 1.00. Taking the density of Pb–Sn eutectic as 8.45×10^3 kg m^{-3} gives a discharge coefficient of $C_D = 1.02$; this value is sufficiently close to

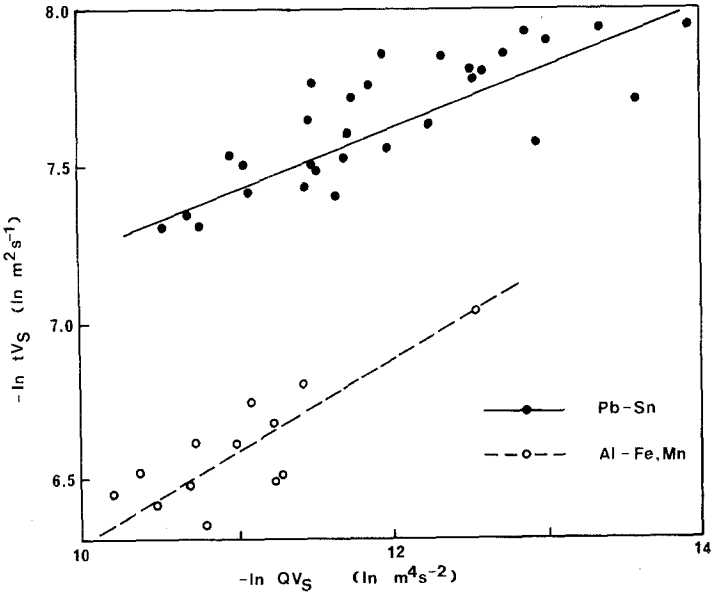

Figure 3 Ribbon thickness t for melt-spun Pb–Sn eutectic and Al alloys as a function of volumetric flow rate Q and surface velocity of the drum V_S, following the analysis of Kavesh [4]. The points show the experimental data and the lines show the least-squares best fit.

unity that the results are virtually identical to those obtained by Liebermann and Graham. Taking the density of Al as 2.71×10^3 gives $C_D = 0.76$ and this rather low value may reflect the rather poor flow characteristics which were exhibited by the Al alloys during melt-spinning.

Kavesh [4] used a more detailed analysis of thermal and momentum transport during melt-spinning to obtain independent equations for the width and thickness of melt-spun ribbons

$$\ln (wV_S) = c + n \ln (QV_S) \quad (3)$$

$$\ln (tV_S) = -c + (1-n) \ln (QV_S), \quad (4)$$

where c is a constant depending upon the thermal characteristics of the solidifying material, and n is a constant in the range 0.75 to 1.00. Data for amorphous $Fe_{40}Ni_{40}B_{20}$ agreed well with Equation 3 and somewhat less well with Equation 4, with $n \sim 0.85$. The present results for Pb–Sn eutectic and Al–2%(Fe,Mn) are shown in Figs. 2 and 3. Once again, there is good agreement in Fig. 2 for the width variation predicted in Equation 3, but poorer agreement for the thickness data shown in Fig. 3. Linear regression analysis of the Pb–Sn width data gives $n = 0.81$ and $c = 5.4$ with a correlation coefficient of 0.99; the thickness data for Pb–Sn also gives $n = 0.81$ and $c = 5.4$ with a correlation of only 0.80. For the Al alloys, width measurements give $n = 0.93$ and $c = 6.4$ with a correlation coefficient of 0.95; however, the thickness results do not agree so well, giving $n = 0.75$ and $c = 3.8$ with a correlation of 0.80. Once again, the poorer results for Al alloys may be a result of their poor flow characteristics and a tendency for fibrilation during melt spinning.

Liebermann [6] has recently pointed out that there is an empirical relationship between ribbon with width w and volumetric flow rate Q in a variety of melt-spun Fe–Ni based amorphous alloys

$$w = w_o + Q\nu_p, \quad (5)$$

where w_o and ν_p are constants. Liebermann interpreted ν_p as an average dynamic viscosity in the solidifying liquid, and found that its value was approximately constant at 1.0 to 1.1×10^{-3} m^2 sec^{-1} for the range of alloys that he studied. Data for Pb–Sn eutectic and Al–2%(Fe,Mn) are shown in Fig. 4, and for both types of alloy agreed with Equation 5 within a correlation coefficient of 0.96. The values of ν_p are 0.66×10^{-3} m^2 sec^{-1} for Pb–Sn and 0.77×10^{-3} m^2 sec^{-1} for Al–(Fe,Mn), in both cases lower than the values found by Liebermann. However, this difference is not unreasonable; in an amorphous alloy the liquid viscosity rises sharply just ahead of the solidification front, but there is no equaivalent increase in viscosity ahead of a crystallizing interface.

The present results can be summarized as showing that the analyses of Liebermann and Graham, Kavesh, and Liebermann can be extended reasonably well from amorphous Fe–Ni based alloys to the rather different cases of crystalline

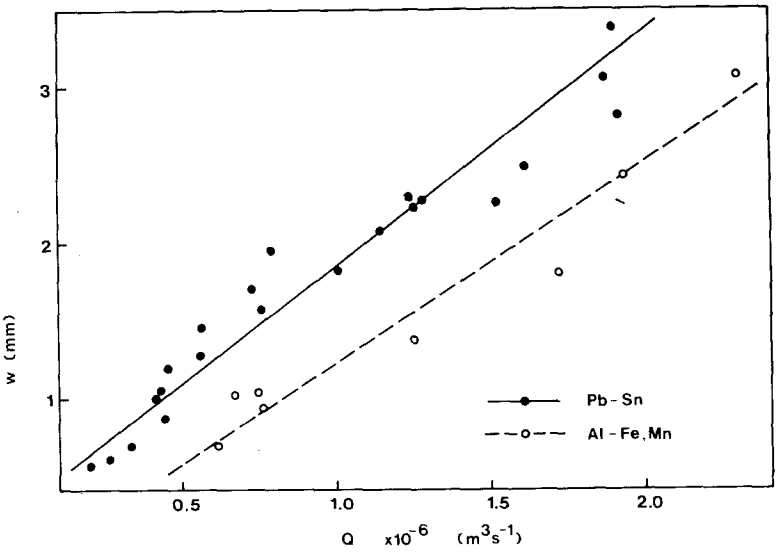

Figure 4 Ribbon width w for melt-spun Pb–Sn eutectic and Al alloys as a function of volumetric flow rate Q, following Liebermann's empirical relationship [6]. The points are the experimental data and the lines show the least-squares best fit.

Pb–Sn eutectic and low content Al alloys. However, there are three reservations. Firstly, a discharge coefficient must sometimes be included in Liebermann and Graham's analysis of ribbon cross-sectional area, to allow for inefficient ejection at the orifice. Secondly, there is considerable scatter in the variation of ribbon thickness, although the average trend is still in quite good agreement with Kavesh's analysis. Thirdly, the liquid viscosity in Liebermann's empirical relation for ribbon width is considerably lower in a crystallizing alloy compared to the amorphous alloys studied previously.

Acknowledgements

The authors would like to thank the UK Science Research Council and US Office of Naval Research (N-00014-789-00) for providing financial support for this research programme, and Professor R. W. Cahn for providing laboratory facilities.

References

1. P. DUWEZ, R. H. WILLENS and W. KLEMENT Jr., *J. Appl. Phys.* **31** (1960) 1136.
2. "Rapidly Quenched Metals" edited by B. Cantor (Metals Society, London, 1978).
3. H. H. LIEBERMANN and C. D. GRAHAM, *IEEE Trans. on Magnetics MAG-12* (1976) 921.
4. S. KAVESH, "Metallic Glasses" edited by J. J. Gilman and H. J. Leamy (ASM, Metals Park, Ohio, 1976) p. 36.
5. R. CHEESE and B. CANTOR, *Mater. Sci. Eng.* **45**.
6. H. H. LIEBERMANN, *Mater. Sci. Eng.* to be published.

Received 18 January
and accepted 30 January 1980.

S. J. B. CHARTER,
D. R. MOONEY,
R. CHEESE,
B. CANTOR,
School of Engineering and Applied Sciences,
University of Sussex,
Falmer, Brighton
Sussex, UK

The strength of α-sialon ceramics

A new member of sialon ceramics, which has the α-Si_3N_4 structure, has been considered in recent publications [1–3]. The general formula for α-sialon, $M_n(Si, Al)_{12}(O, N)_{16}$ where M = Li, Mg, Ca, or Y and $n \leqslant 2$, shows that the M ion dissolves at interstitial sites. There are two interstitial sites for the dissolution in a unit cell of α-sialon [1].

The reaction for α-sialon formation is shown by Y-α-sialon with, for example,

$$Si_3N_4 + a(Y_2O_3 + 9AlN) \rightarrow$$

$$Y_{2a}(Si_3, Al_{9a})(O_{3a}, N_{4+9a}),$$

where $a \leqslant 1$. The end member for the reaction, $(Y_2O_3 + 9AlN)$, corresponds to $Y_2(Al_9)(O_3, N_9)$ although the compound was not formed by the reaction of Y_2O_3 and AlN. The equation shows that the metal to non-metal ratio (M/X) is kept constant (3/4) in the network of α-sialon. There is no vacant site in the network of α-sialon formed by the (Si, Al)(O, N)$_4$ tetrahedron as in β-sialon ($Si_{6-z}Al_zO_zN_{8-z}$, $0 < z \leqslant 4.2$). But when interstitial sites are partly occupied by metal ions, the rest can be regarded as vacant sites which may allow ionic conduction [4]. The other characteristic of α-sialon is a low oxygen content compared with that in β-sialon [1]. α-sialon ceramics have potential for application as electrical or mechanical materials at high temperatures, but as far as we know, there have been no reports on the properties of α-sialon. The present communication reports on the strength of hot-pressed (HP) and reaction-sintered (RS) Y-α-sialon. The composition used in the present work was $Y_{0.41}(Si_{10.2}Al_{1.8})(O_{0.6}, N_{15.4})$.

Hot-pressed α-sialon was obtained by heating the powder mixture (Si_3N_4* 50, Y_2O_3† 3, and

TABLE I The Composition of α-sialon

	Y	Si	Al	O	N
Calc	0.41	10.2	1.8	0.6	15.4
Obs	0.45	9.5	2.5	1.0	14.9

*H. C. Starck, W. Germany.
†Shin-etsu Chemical, Japan.

